JOINT INSTITUTE FOR NUCLEAR RESEARCH
Dzhelepov Laboratory of Nuclear Problems

FINAL REPORT ON THE SUMMER STUDENT PROGRAM

Monte-Carlo simulation and image reconstruction for Medipix-based coded aperture gamma camera

Supervisor:
Chelkov Georgy Alexandrovich

Student:
Rastorguev Daniil, Russia
MIPT

Participation period:
July 22 – August 31

Dubna, 2018

Abstract

A gamma camera prototype which uses coded aperture imaging technique and position-sensitive Medipix detector was simulated with Geant4 toolkit. Decoding software, based on simple back projection algorithm, was developed to reconstruct the image in the near field.

1 Introduction

Gamma sources exact locating is crucial in such fields as nuclear decommissioning, X-ray astronomy, emission tomography. To increase the efficiency, detection systems should have sufficient spatial resolution to determine gamma source position properly. Such spatial-resolved detection systems (often referred to as imaging systems) require a position-sensitive detector, e.g. photographic film, and a focusing system, which should provide different detector response for sources in different location [1].

For hard X-rays and gamma rays imaging systems should be designed in a special way. Several technologies exist to detect these rays, e.g. special films or position-sensitive scintillators and semiconductor detectors. Due to high penetration ability of these rays they cannot be reflected or refracted, therefore conventional focusing systems based on lenses and mirrors cannot be used.

One of the simplest focusing technologies called pinhole, however, works for gamma rays. A single hole in an opaque plate creates an inverted copy of a real image on the detector. A significant downside of a pinhole is a restriction put on signal-to-noise ratio (SNR) and angular resolution. The smaller pinhole grants better angular resolution, but weaker signal, so it can be overshadowed by detector background noise. And vice versa, larger pinhole grants better SNR but worse resolution. The technology can be improved with adding more holes, forming so-called coded aperture, which allows to significantly increase SNR, keeping the angular resolution [2]. Though, images obtained with such technique, require post-processing with special algorithms. A scheme of gamma camera with coded aperture is represented on Fig. ??

The paper is arranged as follows. Section 2 introduces a concept of gamma imaging system, based on pixelated detector and coded aperture. Section 3 describes Monte-Carlo simulation of a gamma camera prototype. Section 4 is denoted to decoding the data obtained from the simulation. In section 5 results are represented and discussed.

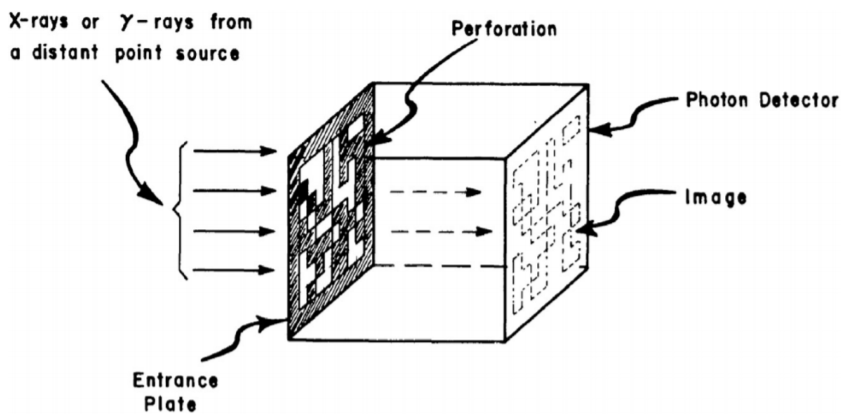

Figure 1: Imaging system with coded aperture

2 Gamma-camera prototype

The gamma camera prototype, which is currently under development in DLNP, is designed for single-photon emission computed tomography (SPECT). The imaging system is to be used for in vivo detection of gamma radiation of specific radiopharmaceuticals.

The camera utilizes Medipix pixelated semiconductor detector which consists of CdTe plate and readout layer. The chip has total resolution of 256×256 pixels (pixel size 55 μm). Each pixel carries dedicated integral circuits which include an amplifier, an analog-to-digital converter and memory. The chip can detect single photons and is capable to measure energy deposit [4].

For the focusing a coded mask aperture is used. The mask has special pattern (Fig. 2), called modified uniformly redundant array (MURA). Masks with such pattern significantly improve SNR by using all the detector plate efficiently and at the same time decrease distortion which occurs at the post-processing stage [3]. The mask is made of tungsten and has thickness of 1 mm. Transparent parts of the pattern are created with holes, cut with high precision laser (Fig. 3). Opaque parts of the plate is able to weaken gamma flux up to 20 times (for 140–160 keV photon energy, which is characteristic for widely used radionuclides ^{99m}Tc and ^{123}I).

Another specific feature of the system is related to MURA masks usage: when the mask is rotated by 90 degrees, all the elements invert (except the central one). This allows to eliminate noise, caused by mask transparency, by taking two shots with different mask orientation. Therefore, the prototype is to be equipped with a revolving mechanism which may lock mask in different positions.

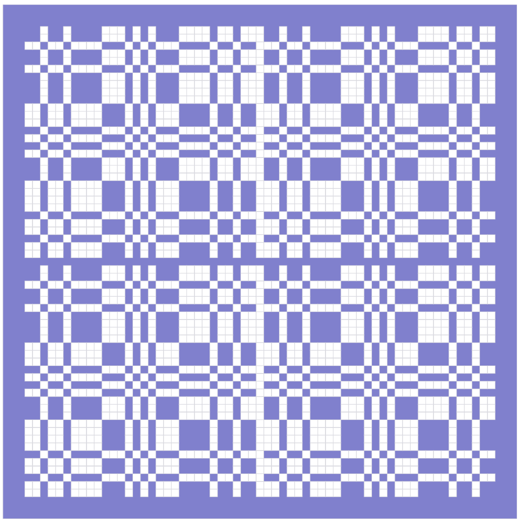

Figure 2: 61 × 61 MURA mask pattern

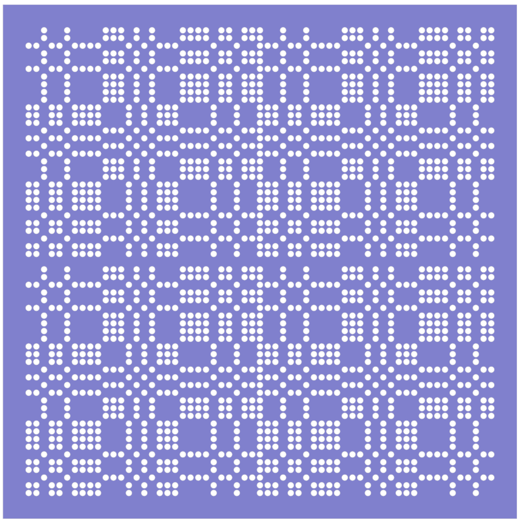

Figure 3: Mask with laser drilled holes

3 Monte-Carlo simulation

A modelling software was developed to simulate the system and test its geometry. Geant4 toolkit was used. Geant4 uses built-in Monte-Carlo algorithm to simulate particles, passing through matter. The toolkit tracks particles separately, providing all the possible information about each track. In this simulation, energy deposit and hit coordinates are measured for particles which hit the Medipix detector. The data gathered is stored in special files using ROOT, a high performance data processing framework.

So far as simulation software grants ability to modify camera and gamma sources geometry, several runs were performed to get detector responses (so-called *shadowgrams*) for different source position and number. Different coding masks were used: an ideal coding mask with square lattice pattern and its real implementation with round holes. The shadowgrams obtained then were used to test the post-processing software.

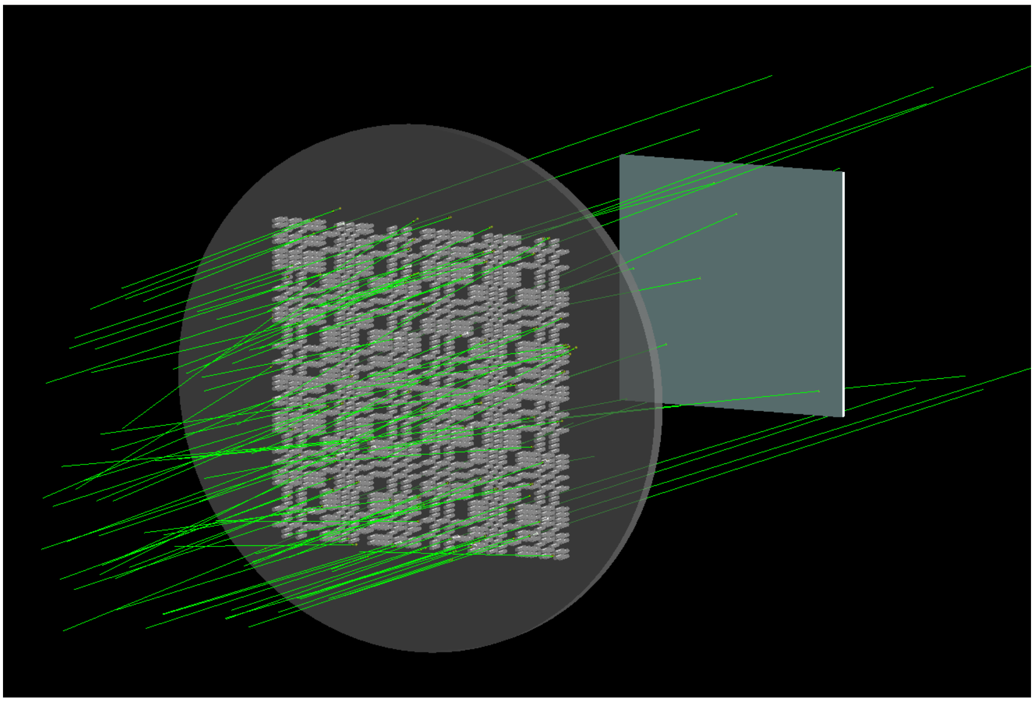

Figure 4: Prototype simulation in Geant4 toolkit

4 Image decoding

The shadowgram, a detector response on a gamma image, contains encoded information about the pictured object but requires post-processing for a visual object representation. Two different algorithms were tested for decoding shadowgrams.

4.1 Decoding array convolution algorithm

According to [2], shadowgram S of object O is formed as follows:

$$S = (O * A) + N, \tag{1}$$

where A and N represent coded aperture and detector background noise accordingly, and "$*$" stands for the *convolution* operation. To reconstruct the object $\tilde{O}$ from the shadowgram, one should convolute it with special decoding array G.

$$\tilde{O} = S * G \tag{2}$$

The decoding array is chosen in way so that $A * G$ approximates a delta function. For real applications continual abstract objects O, S etc. are represented as pixelated images, which can be operated like matrices. For matrices convolution operation takes form:

$$\tilde{O}_{ij} = \sum_{k,l} S_{kl}\, G_{i+k,j+l}. \tag{3}$$

For MURA-type coded mask apertures decoding massive G can be easily calculated, and $A*G$ function is a delta-shaped peak with zero sidelobes, which decreases discrepancy between original object O and reconstructed object $\tilde{O}$ [3].

4.2 Simple back projection algorithm

Consider a flat pixelated image on a certain distance from the aperture (Fig. 5). The resolution is the same as the detector has According to [5], image can be reconstructed from the shadowgram by the following algorithm (represented in pseudocode):

```
for each pixel on detector
    for each pixel on image
         build a line segment which connects detector pixel and image pixel;
         calculate point of intersection of this segment and the mask plate;
         if (mask in this point is opened)
             image pixel value += detector pixel counts;
    end
end
```

This algorithm may be improved, which results increase in accuracy for mask with complicated shapes, for example, MURA mask with holes.

```
for each pixel on detector
    for each pixel on image
         calculate the fraction of detector pixel exposed to image pixel;
         image pixel value += detector pixel counts * fraction;
    end
end
```

However, for the current setup, where image and detector pixels are significantly smaller than mask pattern elements, `fraction` mostly appears to be exact 0 or 1, so the improved algorithm does not differ from the basic one. As the `fraction` calculation is difficult, use of this algorithm is inexpedient.

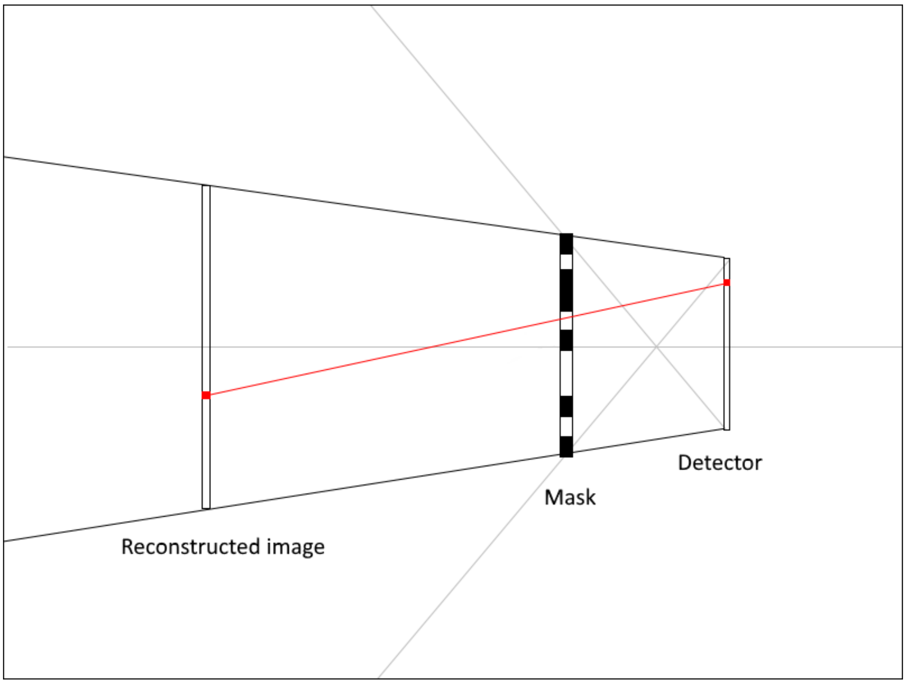

Figure 5: Simple back projection algorithm

After several tests, simple back projection algorithm was chosen over convolution algorithm. Since both algorithms have similar computational complexity $O(n^4)$, (both detector and image have $n \times n$ resolution), back projection is more intuitive. Moreover, it is much more flexible and may be easily adapted to different gamma camera setups.

5 Results

Several shadowgrams were obtained and then decoded with simple back projection algorithm. The decoding algorithm was adjusted to reconstruct image from a 30×30 mm area at the distance of 120 mm from the aperture (see Fig. 5).

5.1 Point sources

A shadowgram for two point sources was obtained and them processed (Fig. 6, 7). Though several visual artifacts at the center of the reconstructed image emerge, peaks location on the reconstruction exactly matches point sources position in the simulation. Measuring peaks FWHM allows to estimate spatial resolution of the system. With Fig. 7 one can estimate resolution to be up to 0.5 mm.

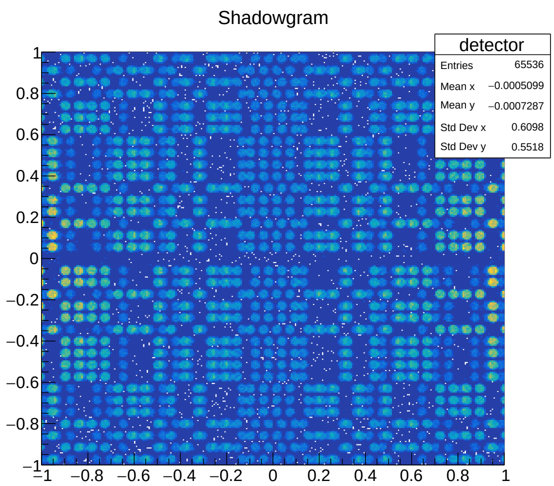

Figure 6: Shadowgram of two point sources (mask with round holes)

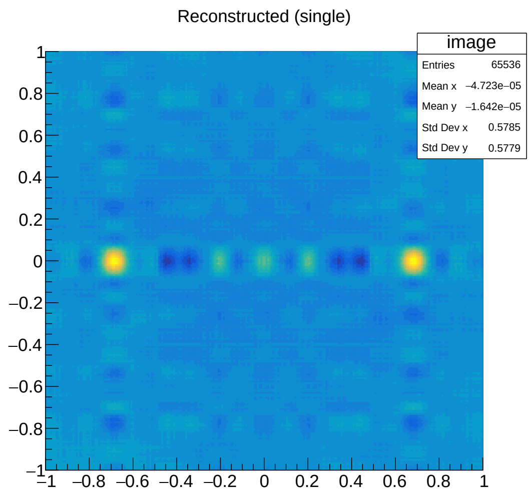

Figure 7: Reconstructed image of two point sources

5.2 Continious source

Shadowgrams for a flat continious source were also obtained. As in previous subsection, the circle-shaped source (1 cm radius) is located in plane at the distance of 120 mm from the aperture (Fig. 8).

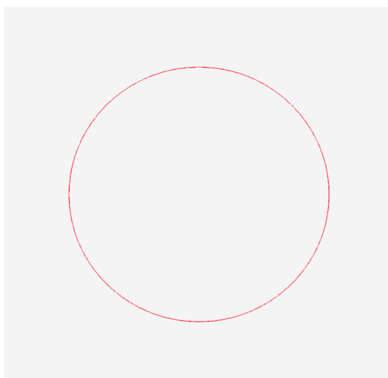

Figure 8: Continious source

To estimate feasibility of laser-drilled holes mask usage, simulation was performed for both ideal and real mask patterns (Fig. 9 and Fig. 10 correspondingly).

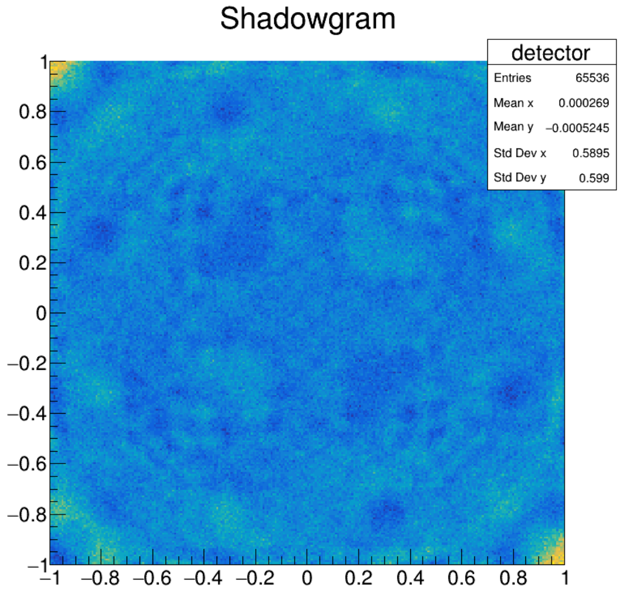

Figure 9: Shadowgram of a circle-shaped source (ideal rectangular MURA)

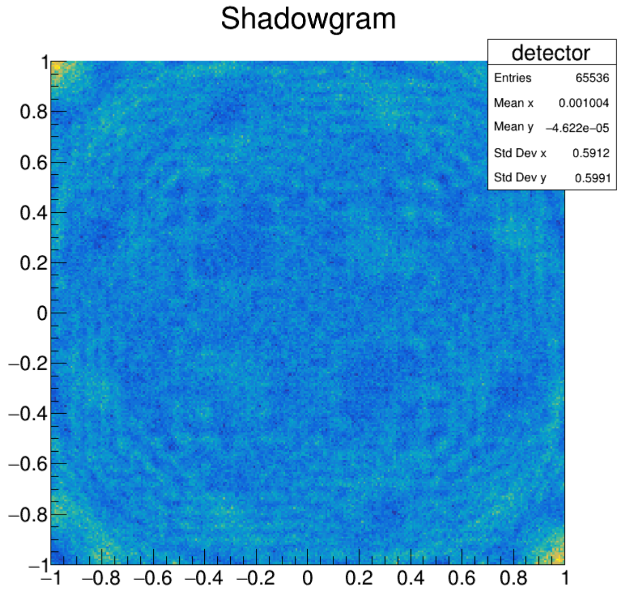

Figure 10: Shadowgram of a circle-shaped source (mask with round holes)

After reconstruction images obtained with different masks are resemblant. However, detailed analysis shows that the image from ideal mask (Fig. 11) has less background noise than the one from real mask (Fig. 13). Also significant background noise and visual artifacts emerge on both images.

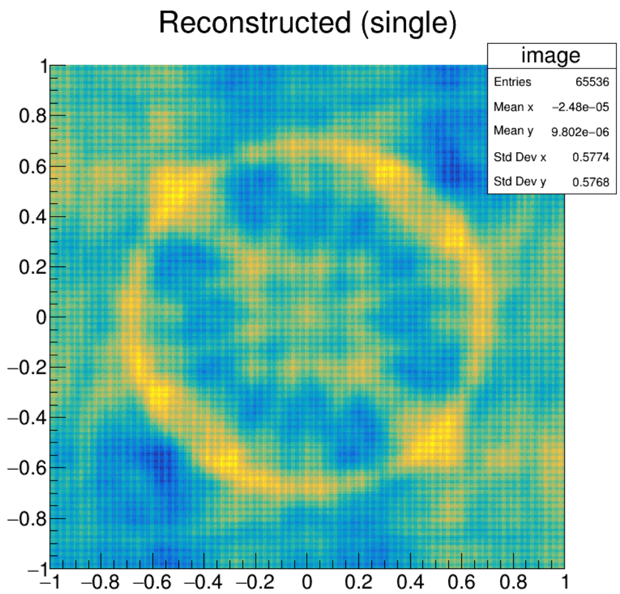

Figure 11: Reconstructed image (ideal rectangular MURA)

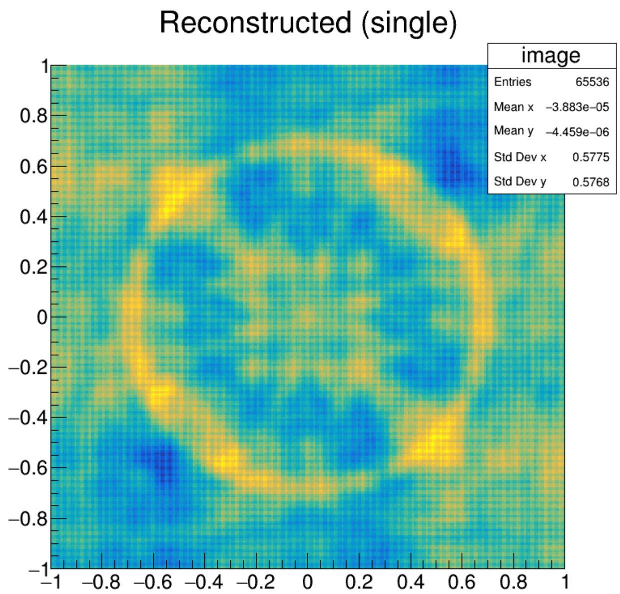

Figure 12: Reconstructed image (mask with round holes)

Dual imaging technique with mask rotation (see Sec. 2) may be used to reduce background noise. Another shadowgram for the rotated mask was obtained during additional simulation, and then image was reconstructed with two shadowgrams. As it is represented on Fig. 14, image reconstruction with two shadowgrams significantly improves SNR by reducing background noise, amplifying the signal and eliminating several visual artifacts. However, some other artifacts (dots at the center) are not eliminated but amplified.

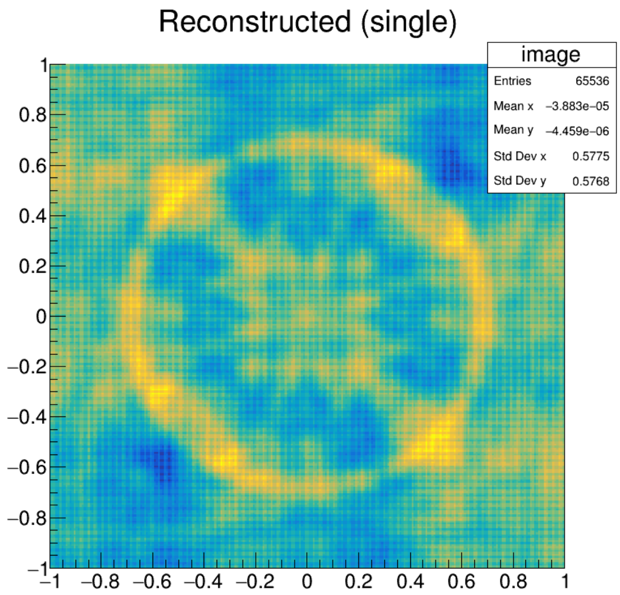

Figure 13: Reconstructed image (single)

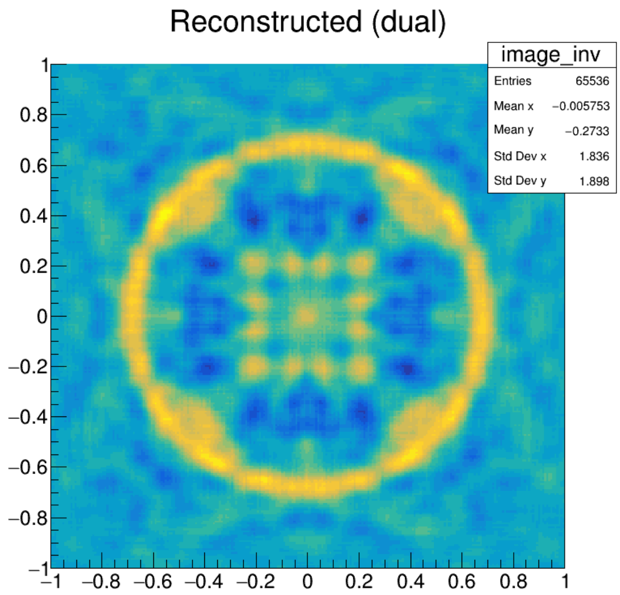

Figure 14: Reconstructed image (dual)

6 Acknowledgements

I would like to express appreciation to my supervisor G. A. Chelkov for his mentorship. Also, advice and professional guidance by D. A. Kozhevnikov have been a great help. In addition, I would like to thank JINR University Centre for the financial support.

References

[1] Michal J. Cieslak et al (2016). Coded-aperture imaging systems: Past, present and future development – a review. *Radiation measurements* 92, p. 59–71.

[2] E. E. Fenimore, T. M. Cannon (1978). Coded aperture imaging with uniformly redundant arrays. *Appl. Opt.* 17, p. 337–347.

[3] Stephen R. Gottesman, E. E. Fenimore (1989). New family of binary arrays for coded aperture imaging. *Appl. Opt.* 28, p. 4344–4352.

[4] X. Llopart et al (2007). Timepix, a 65k programmable pixel readout chip for arrival time, energy and/or photon counting measurements. *Nucl. Instr. and Meth. A* 581, p. 485–494.

[5] Sonal Joshi (2014). Coded Aperture Imaging Applied to Pixelated CdZnTe Detectors (doctoral dissertation). Retrieved from CORE database.